Journal of Neurochemistry

JNC

JOURNAL OF NEUROCHEMISTRY | 2017

doi: 10.1111/jnc.14152

ORIGINAL ARTICLE

Telomerase reverse transcriptase (TERT) – enhancer of zeste homolog 2 (EZH2) network regulates lipid metabolism and DNA damage responses in glioblastoma

Fahim Ahmad,* Shruti Patrick,* Touseef Sheikh,* Vikas Sharma,† Pankaj Pathak,† Prit Benny Malgulwar,† Anupam Kumar,† Shanker Datt Joshi,* Chitra Sarkar† and Ellora Sen*

*Division of Cellular and Molecular Neuroscience, National Brain Research Centre, Manesar, India

†Department of Pathology, All India Institute of Medical Sciences, New Delhi, India

Abstract

Elevated expression of enhancer of zeste homolog 2 (EZH2), a histone H3K27 methyltransferase, was observed in gliomas harboring telomerase reverse transcriptase (TERT) promoter mutations. Given the known involvement of TERT and EZH2 in glioma progression, the correlation between the two and subsequently its involvement in metabolic programming was investigated. Inhibition of human telomerase reverse transcriptase either pharmacologically or through genetic manipulation not only decreased EZH2 expression, but also (i) abrogated FASN levels, (ii) decreased *de novo* fatty acid accumulation, and (iii) increased ataxia-telangiectasia-mutated (ATM) phosphorylation levels. Conversely, diminished TERT and FASN levels upon siRNA-mediated EZH2 knockdown indicated a positive correlation between TERT and EZH2. Interestingly, ATM kinase inhibitor rescued TERT inhibition-mediated decrease in FASN and EZH2 levels. Importantly, TERT promoter mutant tumors exhibited greater microsatellite instability, heightened FASN levels and lipid accumulation. Coherent with *in vitro* findings, pharmacological inhibition of TERT by costunolide decreased lipid accumulation and elevated ATM expression in heterotypic xenograft glioma mouse model. By bringing TERT-EZH2 network at the forefront as driver of dysregulated metabolism, our findings highlight the non-canonical but distinct role of TERT in metabolic reprogramming and DNA damage responses in glioblastoma.

Keywords: ATM, EZH2, FASN, MSI, TERT.

J. Neurochem. (2017) https://doi.org/10.1111/jnc.14152

Human telomerase reverse transcriptase (hTERT), the catalytic subunit of the telomerase, is required for telomere maintenance and cancer cell immortalization. TERT promoter mutation creates a putative binding site for E26 transformation-specific/ternary complex factors (Ets/TCF) transcription factors that promotes enhanced telomerase expression and activity (Huang *et al.* 2013). The prevalence of TERT promoter mutations associated with enhanced expression of telomerase is remarkably high in adult glioblastomas (GBMs) (Killela *et al.* 2013). We have recently demonstrated that inhibition of hTERT not only induces glioma cell apoptosis, but also abrogates pentose phosphate pathway (PPP) (Ahmad *et al.* 2016). The PPP provides NADPH required for fatty acid synthesis (Kather *et al.* 1972), as well as substrates for RNA synthesis and co-factors for *de novo* lipogenesis (Summermatter *et al.* 2010). Fatty acid synthase (FASN), a key metabolic enzyme involved in *de novo* lipogenesis, is over-expressed in gliomas (Grube *et al.* 2014). The

Received May 31, 2017; revised manuscript received July 29, 2017; accepted August 11, 2017.

Address correspondence and reprint requests to Ellora Sen, National Brain Research Centre, Nainwal Mode, NH-8, Manesar 122051, Haryana, India. E-mail: ellora@nbrc.ac.in

Abbreviations used: (p)ATM, (phospho) ataxia-telangiectasia mutated; ChIP-seq, chromatin immunoprecipitation sequencing; CIN, chromosomal instability; DDR, DNA damage response; DMEM, Dulbecco's modified Eagle's medium; DMSO, dimethyl sulfoxide; DN-hTERT, dominant negative – human telomerase reverse transcriptase; DSB, double strand breaks; Ets/TCF, E26 transformation-specific/ternary complex factors; EZH2, enhancer of zeste homolog 2; FASN, fatty acid synthase; GBM, glioblastoma; H3K27me3, histone 3 lysine 27 trimethylation; HI-FBS, heat-inactivated fetal bovine serum; HMG-CoA, 3-hydroxy-3-methylglutaryl coenzyme-A; MMR, mismatch repair response; MSH2, MutS protein homolog 2; MSI, microsatellite instability; MSS, microsatellite stable; MT, mutant; PcG, polycomb group; PGC-1α, peroxisome proliferator-activated receptor gamma coactivator 1-alpha; PPP, pentose phosphate pathway; PRC2, polycomb repressive complex 2; SFM, serum-free media; SREBP-1, sterol regulatory element-binding protein 1; STAT3, signal transducer and activator of transcription 3; TCGA, The Cancer Genome Atlas; TERT/hTERT, (human) telomerase reverse transcriptase; TUNEL, terminal deoxynucleotidyl transferase (TdT) dUTP nick-end labeling; WT, wild type.

importance of FASN in contributing to tumor progression has been demonstrated by the ability of pharmacological inhibitors of FASN to trigger tumor cell apoptosis (Flavin *et al.* 2010). Although dysregulated metabolism, including aberrant lipid metabolism, is recognized as a hallmark of various cancers, little is known about the involvement of TERT in the regulation of lipid metabolism in GBM. Given the known link between PPP and lipogenesis, and our recent findings that hTERT regulates PPP in glioma, we investigated the involvement of TERT in fatty acid metabolism.

The methyltransferase polycomb group protein enhancer of zeste homolog 2 (EZH2), the catalytic factor of the polycomb repressive complex 2 (PCR2), regulates gene expression by methylating lysine 27 on histone H3 (H3K27me3) (Sparmann and van Lohuizen 2006). H3K27me3 is necessary for polycomb repressive complex 2-mediated gene repression (Cao *et al.* 2002). High expression of EZH2 has been linked to progression of several malignancies (Varambally *et al.* 2002; Kleer *et al.* 2003). EZH2 is highly expressed in GBM as compared to low-grade gliomas (Orzan *et al.* 2011), with EZH2–STAT3 (signal transducer and activator of transcription 3) interaction promoting tumorigenicity of glioma stem cells (Kim *et al.* 2013). To investigate the H3K27me3 targets and their relationship with gene expression in astrocytic tumors, we have recently used genome-wide chromatin immunoprecipitation sequencing (ChIP-seq) analysis to evaluate the status of EZH2-mediated H3K27me3 target genes in adult high-grade GBMs with respect to normal brain and low-grade gliomas. This high-resolution genome-wide mapping of H3K27me3 modification has shown higher enrichment of H3K27me3 targets in glioma stem cells of GBMs as compared to diffuse astrocytomas (Sharma *et al.* 2016). Importantly, the chromatin states of wild-type and mutant TERT promoters in several cancer cell lines differ, with mutant and wild-type TERT promoter exhibiting H3K4me2/3 and H3K27me3 mark of active and silenced chromatin, respectively (Stern *et al.* 2015). H3K27me3 epigenetic mark on the promoter of lipogenic genes affects their expression (Podrini *et al.* 2015), and FASN-mediated *de novo* lipid biosynthesis promotes glioma tumor growth and invasion (Yasumoto *et al.* 2016). Interestingly, FASN inhibition enhances DNA damage response (Zeng *et al.* 2008). Elevated EZH2 expression in breast tumor initiating cells increases genomic abnormality (Chang *et al.* 2011), and EZH2 is an (phospho) ataxia-telangiectasia-mutated (ATM) target (Li *et al.* 2013). Moreover, short telomeres elicit genome-wide DNA hypomethylation and altered H3K27me3 levels (Pucci *et al.* 2013).

Transcriptional regulation is dependent on a vast network of epigenetic modifications, and H3K27me3 mark catalyzed and maintained by EZH2 affects local pattern of enrichment and consequently gene expression. Although the links between EZH2, H3K27me3 repressive mark and gene expression have been extensively explored, the involvement of EZH2 in regulation of lipid metabolism in the context of glioma has not been studied. As remodeling of the epigenetic landscape by EZH2 affects gene expression, and since targeting of mutation driven TERT reactivation in glioma has immense therapeutic implications (Li *et al.* 2015), we investigated the correlation between TERT and EZH2, and subsequently the mechanistic links between genes involved in lipid metabolism and DNA repair pathways.

Materials and methods

Cell culture and treatment

Human glioma cell lines A172 (ATCC Cat # CRL-1620; RRID: CVCL_0131) and U87MG (ATCC Cat # HTB-14; RRID: CVCL_0022) obtained from American Type Culture Collection (ATCC, Manassas, VA, USA) were cultured in Dulbecco's modified Eagle's medium supplemented with 10% heat-inactivated fetal bovine serum (HI-FBS) (Cat # 16140071; Gibco, Rockville, MD, USA) and penicillin (100 U/mL)/streptomycin (100 μg/mL) (Cat # 15140122; Gibco). The cells were passaged for fewer than 6 months after resuscitation. On attaining semi-confluence, cells were switched to serum-free media for 4 h and treated with costunolide (30 μM) [(Cat # 2483; Tocris Bioscience, Bristol, UK) for 24 h. Similarly, cells were treated with betulin (100 μM) (Cat # 92648; Sigma-Aldrich, Darmstadt, Germany)]. Cells were pre-treated with ATM kinase inhibitor KU60019 (2.5 mM) (Cat # 2483; Tocris Bioscience) for 2 h in serum-free media followed by treatment with costunolide in the presence or absence of KU60019 for 24 h. Dimethyl sulfoxide (DMSO) (Cat # D8418; Sigma-Aldrich)-treated cells served as controls.

Transfection

Transfections with duplex hTERT (75 nmol/L) (SMARTpool: ON-TARGETplus TERT siRNA L-003547-00-0005) and EZH2 (50 nmol/L) (SMARTpool: ON-TARGETplus EZH2 siRNA L-004218-00-0005) specific siRNAs, and non-specific (NS) siRNAs (siGENOME Non-Targeting siRNA #3 D-001210-03-20 20) or with over-expression constructs for dominant negative-hTERT (DN-hTERT) (Plasmid #1775; Addgene, Cambridge, MA, USA), peroxisome proliferator-activated receptor gamma coactivator 1-alpha (PGC-1α) (Plasmid #10974; Addgene) or corresponding empty vectors (E.Vectors) were carried out using Lipofectamine RNAi Max reagent (Cat # 13778150) or Lipofectamine 2000 reagent (Cat # 11668027) (Invitrogen, Waltham, MA, USA) in Opti-MEM (Cat # 51985034; Gibco) as described previously (Ghosh *et al.* 2013). Cells transfected with NS or specific siRNA, and expression vectors or empty vectors were either harvested 24 h post-transfection or treated with costunolide for additional 24 h. Control non-targeting siRNA as well as siRNAs targeting hTERT and EZH2 were obtained from Dharmacon (Lafayette, CO, USA).

Generation of heterotypic glioma xenografts

Heterotypic xenografts were generated as described previously. Briefly, U87MG cells were injected subcutaneously in the flank of 25 anesthetized athymic nude mice. When measurable tumors, 5–6 mm in diameter, were formed after 15 days of injection, animals were arbitrarily divided into two groups of eight each (including both males and females) and were treated with either vehicle or

costunolide intraperitoneally (5 mg/kg body weight) on alternate days for 20 days, following which they were killed and xenograft tumor tissues were processed for subsequent experiments (Ahmad *et al.* 2016). The mice which did not present with tumors of 5–6 mm diameter (9 in number) after 15 days of injection were excluded from the study. No sample size calculation was performed. The animals were procured from National Institute of Nutrition, Hyderabad, India (RRID not available). All the experimental procedures were in accordance with the guidelines of the Institutional Animal Ethics Committee of NBRC (Approval No. NBRC/IAEC/2013/86).

Determination of cell viability

Viability of cells treated with different concentrations of betulin was assessed using MTS assay (Cat # PR-G3580; Promega, Madison, WI, USA), as described previously (Dixit *et al.* 2009). Values were expressed as percentage change compared to controls.

Western blot analysis

Western blot analysis was performed on protein lysates isolated from control and transfected/treated cells and tumor tissues as described previously (Tewari *et al.* 2012) using antibodies against EZH2 (Cat # ab3748; Abcam, Cambridge, UK; RRID:AB_304045), H3K27me3 (Cat # ab6002; Abcam; RRID:AB_305237), pATM (phospho S1981) (Cat # ab2888; Abcam), ATM (Cat # ab78; Abcam; RRID:AB_306089), FASN (Cat # 3180S; Cell Signaling, Danvers, MA, USA; RRID:AB_2100796), sterol regulatory element-binding protein-1 (SREBP-1) (Cat # NB600-582; Novus Biologicals, Littleton, CO, USA; RRID:AB_10001575), hTERT (Cat # NB120-32020; Novus Biologicals; RRID:AB_805603), PGC-1α (Cat # NBP1-04676; Novus Biologicals; RRID:AB_1522118), MutS protein homolog 2 (MSH2) (Cat # sc-494; Santa Cruz Biotechnology, Santa Cruz, CA, USA; RRID:AB_631975), c23 (Cat # sc-55486; Santa Cruz Biotechnology; RRID:AB_670272) and β-Actin (Cat # A3854; Sigma-Aldrich; RRID:AB_262011). Horseradish peroxidase-labeled secondary antibodies – anti-rabbit IgG (Cat # PI-1000; RRID:AB_2336198) and anti-mouse IgG (Cat # PI-2000; RRID:AB_2336177) were purchased from Vector Laboratories, Inc. (Burlingame, CA, USA). Images were captured using Chemigenius Bioimaging System (Syngene, Bangalore, India) after the addition of chemiluminescent horseradish peroxidase substrate (Cat # WBULS0500; Merck Millipore, Billerica, MA, USA).

Oil red staining

Oil red (Cat # sc-203749; Santa Cruz Biotechnology) staining was performed on frozen sections of control and costunolide-treated xenograft tumors, and on histologically confirmed TERT-mutant and wild-type GBM tissues as described previously (Mehlem *et al.* 2013). Images were captured under Leica DMRXA2 bright-field microscope (Wetzlar, Germany).

Immunohistochemistry

Immunohistochemistry was performed to detect the localization of MSH2 in histologically confirmed TERT-mutant and wild-type GBM tissues as described previously (Dixit *et al.* 2012). Patient samples were obtained as per the guidelines of Institutional Human Ethics Committee of AIIMS (Reference No. IEC/NP-155/2012 and RP/01/2012).

Quantitative reverse transcriptase-PCR (qRT-PCR) analysis

Quantitative RT-PCR analysis for EZH2, FASN, and PGC-1α expressions was performed in TERT-mutant and wild-type GBM samples that were described previously (Ahmad *et al.* 2016). Briefly, RNA was isolated and cDNA was synthesized using high-capacity cDNA Reverse Transcription kit (Cat # 43-688-14; Applied Biosystems, Inc., Waltham, MA, USA), and real-time PCR was performed in ViiA7 Real Time Thermocycler (Applied Biosystems) for 40 cycles using Power SYBR Green PCR master mix (Cat # 4367659; Applied Biosystems).

The primers used for qRT-PCR are as follows:

EZH2:	Forward 5′-GCCAGACTGGGAAGAAATCTG-3′
	Reverse 5′-TGTGTTGGAAAATCCAAG TCA-3′
FASN:	Forward 5′-CAGAGCAGCCATGGAGGAG-3′
	Reverse 5′-GGTGGACTCCGAAGAAGGAG-3′
PGC-1α:	Forward 5′-GTCACCACCCAAATCCTTAT-3′
	Reverse 5′-ATCTACTGCCTGGAGACCTT-3′
18S:	Forward 5′-GAGGGAGCCTGAGAAAACGG-3′
	Reverse 5′-GTCGGGAGTGGGTAATTTGC-3′

MSI analysis

For microsatellite instability (MSI) analysis, multiplex PCR with five quasi-monomorphic mononucleotide repeat markers (BAT25, BAT26, NR21, NR24, and NR27) was performed as described earlier (Goel *et al.* 2010). Genomic DNA was isolated from formalin-fixed, paraffin-embedded tumor samples with a QIAamp DNA mini kit (Qiagen, Valencia, CA, USA). Each anti-sense primer was end labeled with one of the fluorescent markers FAM, HEX, or NED. Amplified PCR products were run on an ABI Prism 3130 Genetic Analyzer (Applied Biosystems, Foster City, CA, USA). Allelic sizes were determined by Gene-mapper 4.1 (Applied Biosystems). Samples with allelic size variations in fewer than two of the microsatellites were classified as microsatellite stable, while samples with allelic size variations in two or more of the microsatellite markers were considered MSI.

The primers used for MSI analysis are listed as follows:

BAT 26	Sense 5′-CTGCGGTAATCAAGTTTTTAG-3′
	Antisense 5′-AACCATTCAACATTTTTAACCC-3′ FAM labeled
BAT 25	Sense 5′-TACCAGGTGGCAAAGGGCA-3′
	Antisense 5′-TCTGCATTTTAACTATGGCTC-3′ HEX labeled
NR 24	Sense 5′-GCTGAATTTTACCTCCTGAC-3′
	Antisense 5′-TTGTGCCATTGCATTCCAA-3′ NED labeled
NR 21	Sense 5′-GAGTCGCTGGCACAGTTCTA-3′
	Antisense 5′-CTGGTCACTCGCGTTTACAA-3′ FAM labeled
NR 27	Sense 5′-AACCATGCTTGCAAACCACT-3′
	Antisense 5′-CGATAATACTAGCAATGACC-3′ HEX labeled

Quantitation of free fatty acid

Fatty acid level was measured in control, transfected/treated cells, and in xenograft tumor tissues using a fatty acid quantitation kit (Cat # K612; Bio-Vision Inc., Milpitas, CA, USA) according to the manufacturer's instructions.

TUNEL assay

Terminal deoxynucleotidyl transferase (TdT) dUTP nick-end labeling (TUNEL) assay was performed on glioma cells (10^4) treated with betulin as described previously (Ahmad *et al.* 2016) using *In situ* Cell Death Detection Kit, TMR red (Cat # 12 156 792 910; Roche Molecular Biochemicals, Indianapolis, IN, USA, Sigma-Aldrich). Cell death was determined from the ratio of number of TUNEL-positive cells (red) that co-localized with 4′,6-diamidino-2-phenylindole (DAPI; blue) to the total number of cells taken from multiple fields.

Statistical analysis

In *in vitro* experiments, comparisons between groups were performed using paired Student's *t*-test. In *in vivo* experiments, statistical analysis was done using unpaired Student's *t*-test. TERT-mutant or wild-type patient samples were analyzed using Mann–Whitney test. All *p*s < 0.05 were considered significant.

Results

TERT regulates FASN expression and fatty acid accumulation

The ability of SREBP to induce FASN increases the formation of fatty acid and lipid droplets in prostate cancer cells (Huang *et al.* 2012). Our recent studies have indicated that TERT inhibition diminishes flux into PPP in glioma cells (Ahmad *et al.* 2016). As PPP activation provides substrate for RNA synthesis and co-factors for *de novo* lipogenesis (Summermatter *et al.* 2010), the effect of TERT inhibition on lipid metabolism was investigated. Pharmacological inhibition of TERT by costunolide decreased FASN and SREBP-1 levels (Fig. 1a and Figure S1a). A similar decrease was observed upon siRNA-mediated hTERT inhibition (Fig. 1a and Figure S1a), or transfection with DN-hTERT (Fig. 1a and Figure S1a). Also, both pharmacological and genetic inhibition of TERT decreased fatty acid accumulation (Fig. 1b).

TERT inhibition represses PGC-1α

Peroxisome proliferator-activated receptor gamma co-activator 1-alpha (PGC-1α) enhances lipogenesis by increasing FASN (Summermatter *et al.* 2010). Decrease in PGC-1α expression was observed in costunolide-treated cells exhibiting decreased FASN levels (Fig. 2a and Figure S2a). Similar decrease was noted in cells transfected with hTERT siRNA or DN-hTERT (Fig. 2a and Figure S2a).

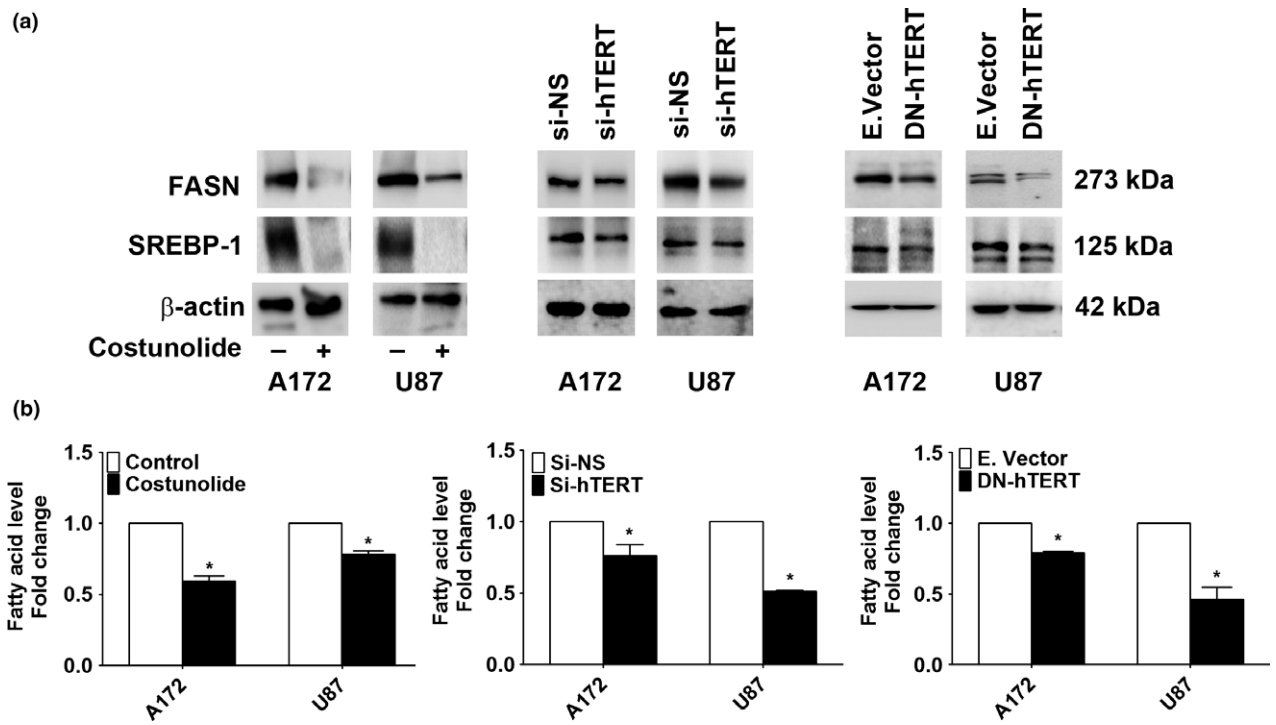

Fig. 1 Telomerase reverse transcriptase (TERT) inhibition decreases fatty acid in glioma cells. (a) Human TERT (hTERT) inhibition decreases fatty acid synthase (FASN) and sterol regulatory element-binding protein-1 (SREBP-1) levels in glioma cells. Western blot images depict diminished FASN and SREBP-1 levels upon pharmacological inhibition of hTERT using costunolide, siRNA-mediated hTERT knockdown, or transfection with DN-hTERT. Blots are representative images of three independent experiments ($n = 3$) showing similar results. Blots were stripped and re-probed for β-actin to establish equivalent loading. (b) Decreased fatty acid levels indicative of lower lipid accumulation in glioma cells upon hTERT inhibition either by costunolide or siRNA or DN-hTERT. Values represent the means ± SEM of three independent experiments ($n = 3$). * denotes significant change from control or mock transfected groups ($p < 0.05$).

Ectopic PGC-1α expression rescues costunolide-mediated decrease in FASN

PGC-1α disruption-mediated telomere dysfunction is attributed to TERT down-regulation (Xiong *et al.* 2015). Diminished FASN expression in costunolide-treated cells is PGC-1α dependent, as ectopic expression of PGC-1α not only rescued costunolide-induced decrease in FASN and SREBP-1 levels (Fig. 2b and Figure S2b), but also prevented costunolide-mediated decrease in fatty acid levels to a significant extent (Fig. 2c). As FASN inhibition triggers tumor cell apoptosis (Flavin *et al.* 2010), the ability of FASN inhibitor betulin to affect glioma cell viability was investigated. Betulin not only induced glioma cell apoptosis (Figure S3a and b), but also abrogated TERT levels (Figure S3c). These results highlight the functional importance of FASN in glioma cell survival.

Elevated EZH2 expression in TERT promoter mutants

Our recent ChIP-seq analysis identified distinct H3K27me3 modification patterns across different grades of astrocytic tumors, without distinguishing between tumors bearing different molecular alterations (Sharma *et al.* 2016). Further analysis of the Chip-seq data set (Sharma *et al.* 2016) for three TERT-mutant and three wild-type tumors indicated

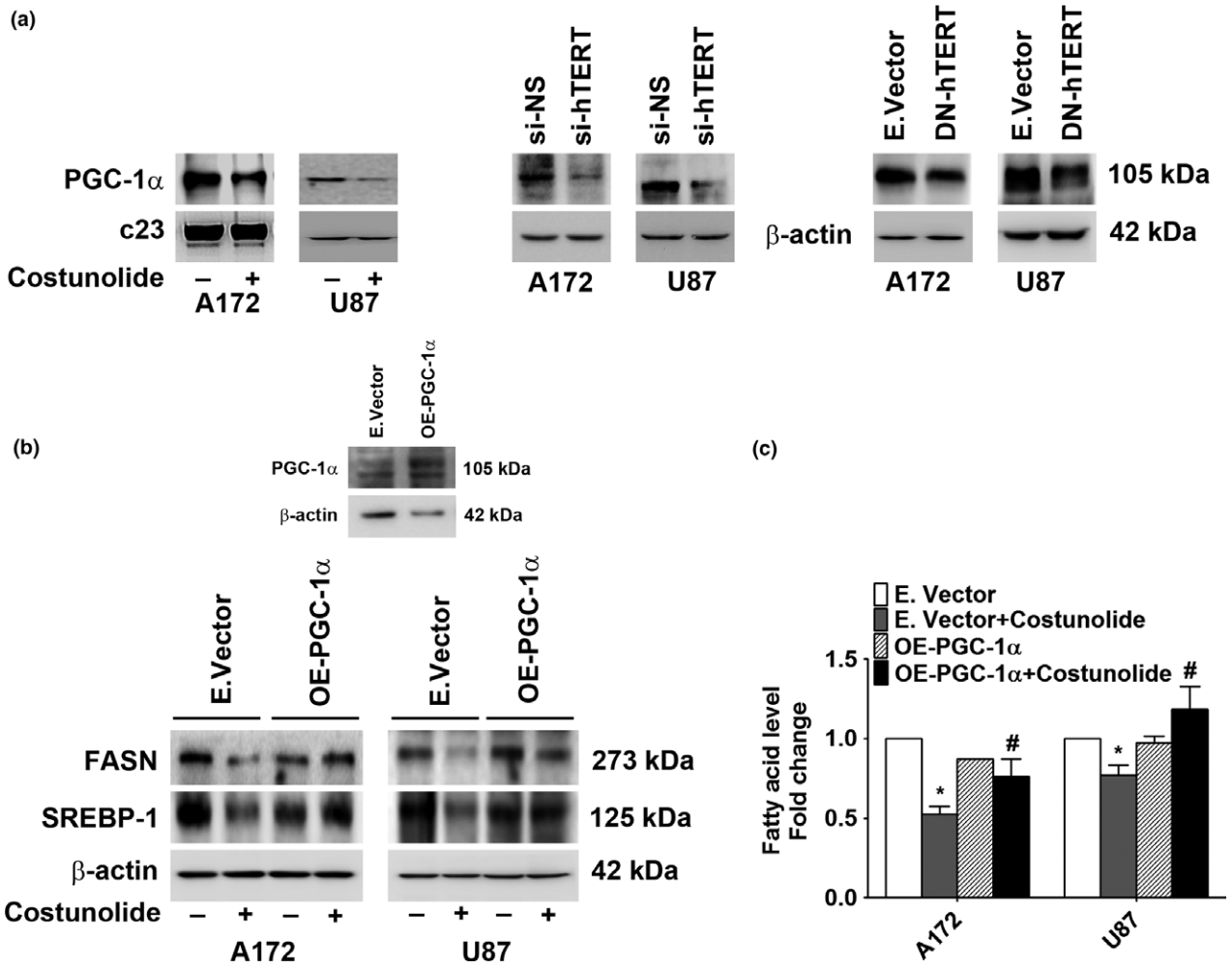

Fig. 2 Fatty acid synthase (FASN) level is regulated by peroxisome proliferator-activated receptor gamma coactivator 1-alpha (PGC-1α) (a) Western blot images demonstrating decreased PGC-1α in glioma cells treated with costunolide, or transfected with human telomerase reverse transcriptase (hTERT) siRNA or DN-hTERT construct. (b) Ectopic PGC-1α over expression rescues costunolide-mediated decrease in FASN and sterol regulatory element-binding protein-1 (SREBP-1) expressions, as demonstrated by western blot analysis. Blots (a and b) are representative images of three independent experiments ($n = 3$) showing similar results. Blots were stripped and re-probed for β-actin or c23 to establish equivalent loading. (c) Ectopic expression of PGC-1α rescues costunolide-mediated decrease in fatty acid levels in glioma cells. Graph represents the change in fatty acid levels in cells transfected with mock or PGC-1α over-expression construct in the presence and absence of costunolide. Values represent the means ± SEM of three independent experiments ($n = 3$). * denotes significant change from mock transfected groups and # depicts significant change from costunolide-treated cells ($p < 0.05$).

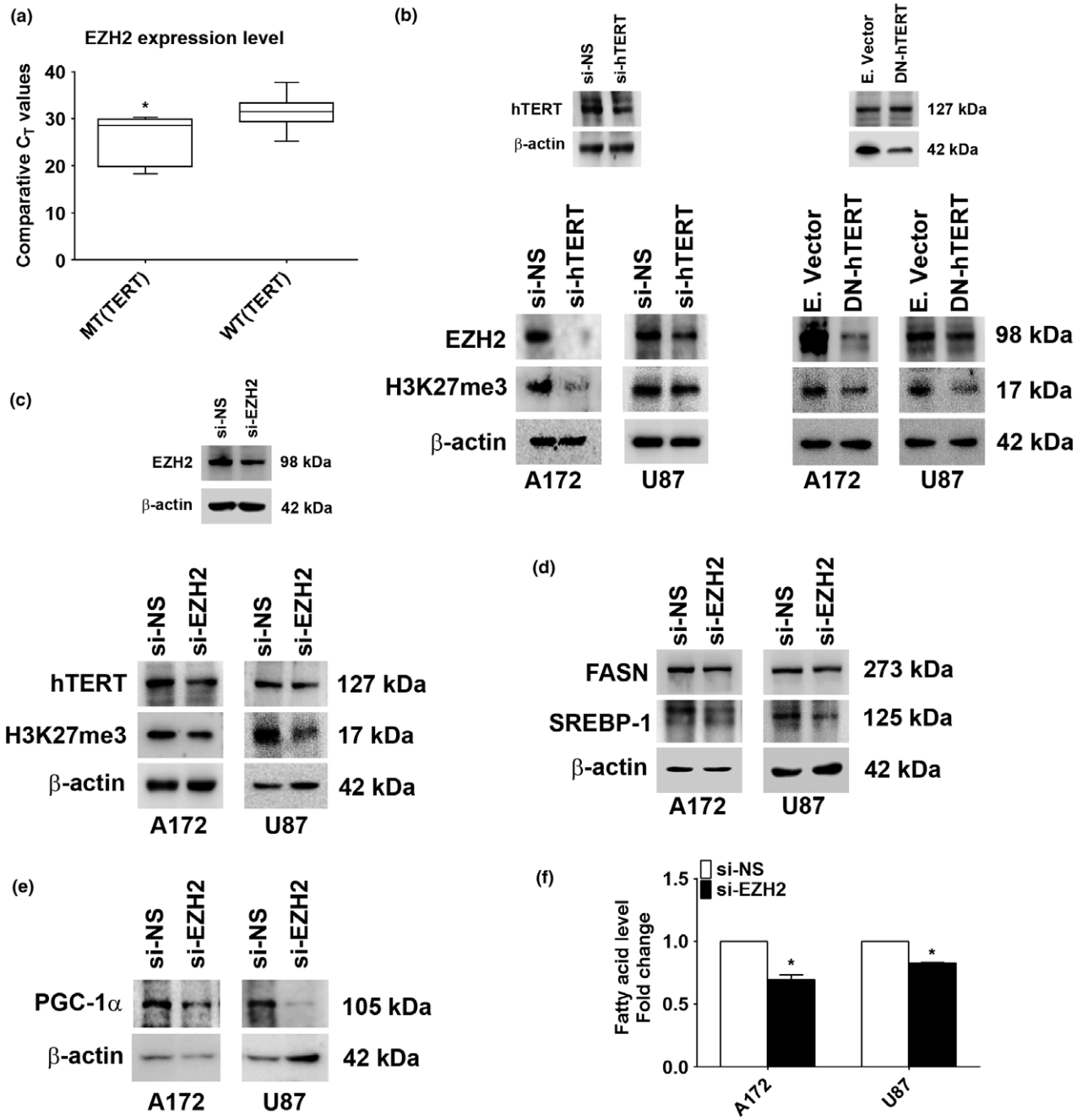

Fig. 3 Existence of telomerase reverse transcriptase (TERT)–enhancer of zese homolog 2 (EZH2) axis in glioma. (a) qRT-PCR indicates an elevated EZH2 transcript level in glioblastoma patients bearing TERT-mutant (MT) ($n = 12$) tumors as compared to TERT wild-type (WT) ($n = 13$) tumors. Results were analyzed using Mann–Whitney test ($p < 0.05$). (b) Inhibition of human TERT (hTERT) in glioma cells with hTERT siRNA or DN-hTERT decreases EZH2 and histone 3 lysine 27 trimethylation (H3K27me3) levels. Insets show the transfection efficiency of hTERT siRNA and DN-hTERT construct (c) siRNA-mediated EZH2 inhibition lowers hTERT and H3K27me3 levels. Inset show the transfection efficiency of EZH2 siRNA (d) Decreased fatty acid synthase (FASN), sterol regulatory element-binding protein-1 (SREBP-1) and (e) Peroxisome proliferator-activated receptor gamma coactivator 1-alpha (PGC-1α) expression in glioma cells upon siRNA-mediated EZH2 knockdown as indicated by western blot analysis. Blots are representative of three independent experiments ($n = 3$) showing similar results. Blots were stripped and re-probed for β-actin to establish equivalent loading. (f) siRNA-mediated knockdown of EZH2 decreases fatty acid levels in glioma cells. Graph represents the change in fatty acid levels expressed as fold change over control in glioma cells transfected with EZH2 siRNA. Values represent the means ± SEM of three independent experiments ($n = 3$). * denotes significant change from control ($p < 0.05$).

lipid metabolism and genomic stability as H3K27me3 targets in GBM bearing hTERT promoter mutations (Figure S4). The targets falling in the protein coding regions were identified and checked for their expression using level 3 The Cancer Genome Atlas expression data of GBM from The Cancer Genome Atlas data portal (http://cancergenome.nih.gov/). Since H3K27me3 modification is involved in mediating gene silencing, we specifically analyzed H3K27me3 targets that had significantly down-regulated levels (Table S1).

Existence of EZH2-TERT axis

EZH2 promotes glioblastoma tumorigenesis and malignant progression through activation of Warburg effect (Pang *et al.* 2016). To understand the correlation between EZH2 and TERT, expression of EZH2 in tumors bearing TERT promoter mutation was investigated. Elevated *EZH2* level was observed in TERT promoter mutant GBM tumors as compared to TERT wild-type tumors (Fig. 3a). A decrease in EZH2 expression was observed upon siRNA-mediated hTERT inhibition (Fig. 3b and Figure S5a) and in cells transfected with DN-hTERT (Fig. 3b and Figure S5a). This was accompanied by decrease in H3K27me3 levels (Fig. 3b and Figure S5a). Conversely, diminished TERT and H3K27me3 expression was observed upon siRNA-mediated EZH2 inhibition (Fig. 3c and Figure S5b). This indicates the importance of TERT–EZH2 crosstalk in sustaining heightened levels of both in TERT mutants.

EZH2 regulates lipid metabolism

Analysis of our ChIP-seq data (Sharma *et al.* 2016) for cases harboring TERT wild-type and mutant indicated PGC-1α to be an EZH2 target in TERT mutants. Since a positive correlation exists between EZH2 and TERT, and as the latter regulates FASN, the involvement of EZH2 in lipid metabolism was investigated. The decrease in FASN and SREBP-1 (Fig. 3d and Figure S5c) as well as PGC-1α levels (Fig. 3e and Figure S5d) observed upon siRNA-mediated EZH2 knockdown was accompanied by diminished fatty acid levels (Fig. 3f).

TERT–EZH2–ATM crosstalk regulates FASN

Lack of telomere protection triggers DNA damage response (DDR) involving phosphorylation of ATM (Blasco 2005), and FASN knockdown diminishes DNA damage (Xiao *et al.* 2008). Besides its involvement in DDR, ATM activates the PPP to promote anti-oxidant defense (Cosentino *et al.* 2011). Importantly, ATM-mediated EZH2 phosphorylation prevents polycomb repressive complex 2 formation and H3K27 methylation (Li *et al.* 2013). As TERT inhibition diminishes FASN, the status of ATM under such conditions was investigated. An increase in pATM levels was observed in costunolide-treated cells (Fig. 4a and Figure S6a). Similar dependence of ATM phosphorylation on hTERT was also evident from elevated pATM levels in cells transfected with TERT siRNA or DN-hTERT (Fig. 4a and Figure S6a). As EZH2 is an ATM target (Li *et al.* 2013), the involvement of the latter in EZH2 regulation was investigated. Treatment with ATM kinase inhibitor (KU60019) prevented costunolide-induced decrease in EZH2 (Fig. 4b and Figure S6b). This increase in ATM phosphorylation is crucial for lipid metabolism, as ATM kinase inhibitor prevented costunolide-mediated changes in FASN, SREBP-1 and PGC-1α (Fig. 4b and Figure S6b). KU60019 also rescued costunolide-mediated decrease in fatty acid accumulation (Fig. 4c). Besides, elevation in pATM level was observed upon EZH2 inhibition (Fig. 4d and Figure S6c). The ability of ATM to negatively regulate lipid metabolism upon TERT inhibition indicates the importance of EZH2–TERT driven DNA damage responses in lipid metabolism.

Correlation between DNA mismatch repair response, ATM, and TERT

Mismatch repair response (MMR) pathway affects telomere function as deficiency of MMR gene MSH2 abolishes the anticancer activity of short telomeres (Martinez *et al.* 2009). High telomere mutation frequency is observed in sporadic colon cancers with MSI and lacking MMR gene MSH2 (Pickett *et al.* 2004). Changes in MSH2 levels strongly predict the response of GBM tumors to temozolomide treatment (McFaline-Figueroa *et al.* 2015). Besides, MSH2 expression can be reversed by simvastatin, a 3-hydroxy-3-methylglutaryl coenzyme-A reductase inhibitor with cholesterol-lowering ability (Floer *et al.* 2008). The decrease in MSH2 level observed upon pharmacological inhibition of TERT was reverted in the presence of KU60019 (Fig. 4e and Figure S6d). EZH2 regulates MSH2 through H3K27me3 (Yang *et al.* 2016), and a decrease in MSH2 level was observed upon siRNA-mediated EZH2 knockdown (Fig. 4f and Figure S6e).

Elevated FASN and PGC-1α in GBM harboring TERT promoter mutations

As our findings indicate a positive correlation between TERT and fatty acid metabolism in glioma cells, the status of FASN in tumors harboring TERT mutations was evaluated. Increased *FASN* mRNA level was accompanied by elevated *PGC-1α* expression in TERT mutants (Fig. 5a and b). Heightened accumulation of lipid droplets and increased MSH2 expression were observed in TERT mutants as compared to wild-type (Figure S7a and b).

Microsatellite instability in TERT mutants

MSI pathway involves a failure of the mismatch repair system, and deficiency of MMR enables cells to overcome crises resulting from critical shortening of telomeres (Bechter *et al.* 2004). Activation of telomerase is frequent in tumors exhibiting MSI (Ibanez de Caceres *et al.* 2004), and FASN

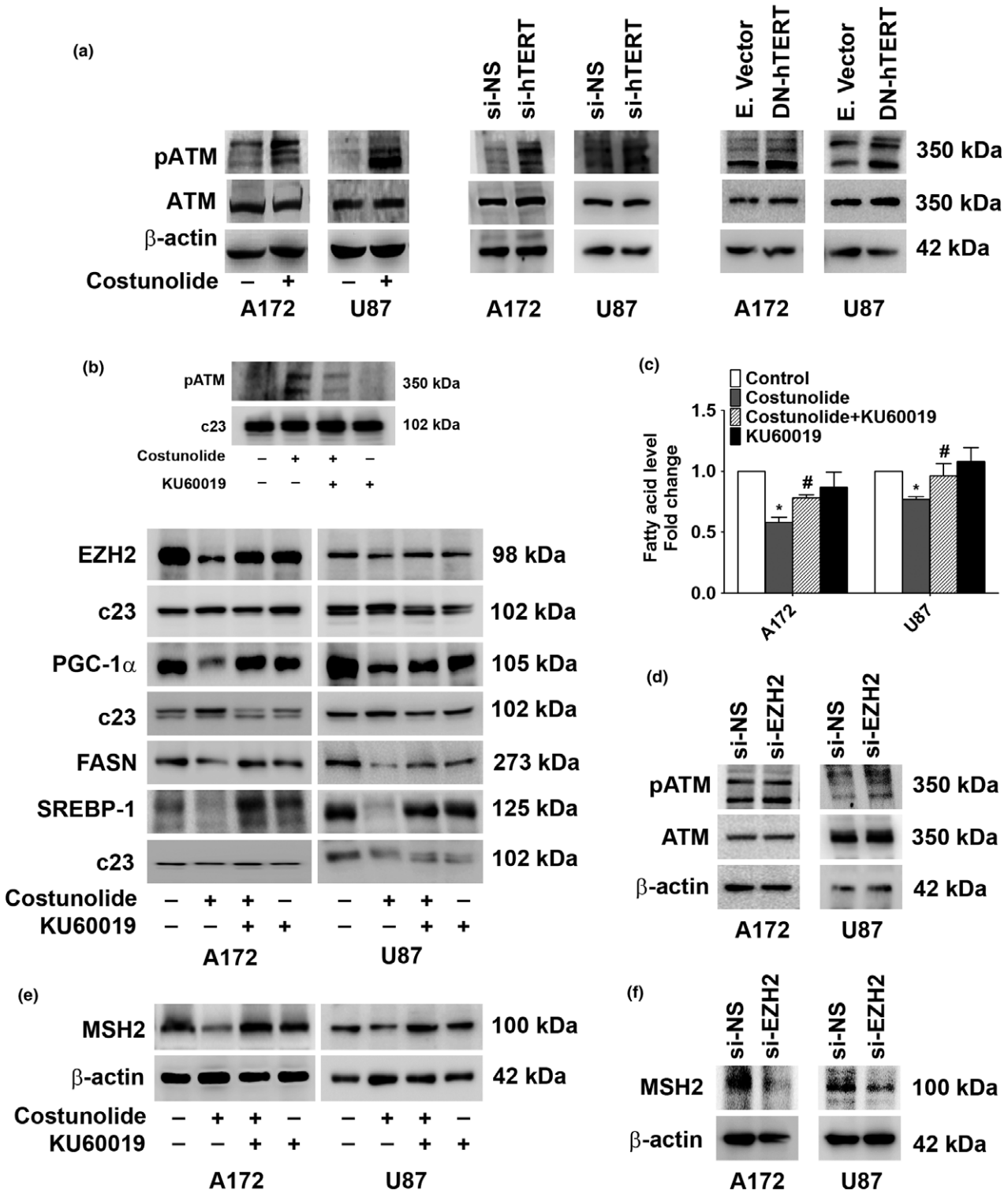

over-expression in colorectal cancer is associated with MSI (Ogino *et al.* 2007). Besides, ChIP-seq analysis revealed chromosomal partitioning as an H3K27me3 target in TERT mutants (Sharma *et al*. 2016). Although MSI and chromosomal instability have been regarded as mutually exclusive, recent evidence suggests overlap between the two (Trautmann *et al.* 2006). As inactivation of any of the several MMR genes, including MSH2 can result in MSI, we

investigated MSI in TERT mutants. We tested a panel of five quasi-monomorphic mononucleotide repeat markers amplified in a single multiplex PCR reaction (pentaplex PCR) to detect MSI. The marker panel consisted of BAT25, BAT26, NR21, NR24, and NR27 markers (Goel *et al.* 2010). Out of patient tumor samples examined, 30% of the TERT mutants were found to be MSI positive, while only 10% of wild types were MSI positive (Fig. 5c and Table S2). Microsatellite status investigated by PCR with three out of five microsatellite markers analyzed showing evidence of instability suggests that TERT mutant tumors are indeed MSI-high (Fig. 5c and Figure S8a,b).

Costunolide affects lipid metabolism in glioma xenograft tumors

Costunolide impairs tumor growth, decreases PPP flux and diminishes TERT expression in treated glioma xenograft (Ahmad *et al.* 2016). On investigating the effect of costunolide on lipid metabolism in xenograft model, decrease in FASN, SREBP-1, and PGC-1α expression (Fig. 6a and Figure S9a), diminished fatty acid levels (Fig. 6b), and lipid droplet accumulation (Fig. 6c) were observed. Costunolide-mediated decrease in EZH2, H3K27me3, and MSH2 levels (Fig. 6d and Figure S9b) were accompanied by increased pATM levels (Fig. 6e and Figure S9c).

Discussion

Telomere dysfunction represses PGC-1α responses and affects mitochondrial biology (Sahin *et al.* 2011). Importantly, PGC-1α plays a pivotal role in progression and metastasis of prostate cancer by modulating the metabolic state of cells (Wallace and Metallo 2016). The dependence of FASN on PGC-1α is known (Summermatter *et al.* 2010), and FASN expression is up-regulated in gliomas (Wakamiya *et al.* 2014). Our findings indicate the dependence of PGC-1α and FASN on telomerase activation in glioma cells. Increased fatty acid synthesis promotes tumorigenesis and drug resistance by negatively regulating the DDR pathway (Zeng *et al.* 2008). The ability of TERT to drive DNA damage responses and lipogenic flux suggests the existence of an important link between DDR and lipid metabolism in glioblastoma. Thus, in addition to performing its known function of counteracting telomere shortening, hTERT also performs a non-canonical function of regulating lipid metabolism and genomic stability in glioma cells.

Regulation of lipogenic genes such as FASN by modulating the association of the repressive H3K27me3 histone marks on their promoters is known (Podrini *et al.* 2015). The chromatin state of wild-type and mutant TERT promoters exhibit different marks of active and silenced chromatin (Stern *et al.* 2015). Also, our recent genome-wide analysis has revealed a higher enrichment of H3K27me3 targets in glioma stem cells of high-grade GBM as compared to low-grade tumors (Sharma *et al.* 2016), and inhibition of EZH2 activity decreases the glioma stem cell tumorigenicity (Natsume *et al.* 2013). Moreover, telomere-shortening-induced altered H3K27me3 enrichment at Nanog promoter affects the ability to repress pluripotency factors critical to stable differentiation of embryonic stem cells (Pucci *et al.* 2013). Elevated EZH2 levels in TERT mutants play a fundamental role in gliomagenesis through epigenetic reprogramming of H3K27me3 modification marks, as EZH2 knockdown not only affected TERT expression but also lipid metabolism. This study has revealed the unanticipated but distinct role of the well-known repressive H3K27me3 mark in regulating lipid metabolism in GBMs harboring distinct molecular alterations. The mechanistic differences between TERT wild types and mutants in terms of this metabolic profile may provide the basis of a rational therapeutic approach.

Depletion of EZH2 decreases the efficiency of DNA double-strand break repair and increases sensitivity of cells to gamma irradiation (Campbell *et al.* 2013). EZH2 overexpression confers Cisplatin resistance in ovarian cancer (Hu *et al.* 2010). Moreover, deficiency of MMR not only enables the cells to overcome crises resulting from critical shortening

Fig. 4 EZH2 regulated ataxia-telangiectasia-mutated (ATM) activation prevents costunolide-mediated decrease in fatty acid synthase (FASN). (a) Western blot images demonstrating increased phosphorylation of ATM (Ser 1981) in glioma cells treated with either costunolide, or transfected with human telomerase reverse transcriptase (hTERT) siRNA or DN-hTERT construct. (b) Inhibition of ATM reverses costunolide-mediated effects on EZH2, peroxisome proliferator-activated receptor gamma coactivator 1-alpha (PGC-1α), FASN, and sterol regulatory element-binding protein-1 (SREBP-1). Western blot analysis depicts expression of EZH2, PGC-1α, FASN, and SREBP-1 in glioma cells treated with costunolide in the presence or absence of ATM kinase inhibitor KU60019. Inset shows the inhibition of ATM phosphorylation upon treatment with KU60019. (c) KU60019 rescues costunolide-mediated decrease in fatty acid accumulation. Graph depicts the change in fatty acid level expressed as fold change over control in glioma cells treated with costunolide, KU60019, or both. Graph represents means of values ± SEM pooled from experiments repeated three times ($n = 3$). * denotes significant change from control and # represents significant change from costunolide-treated cells ($p < 0.05$). (d) siRNA-mediated EZH2 knockdown increases pATM levels. (e) Treatment with KU60019 rescues costunolide-mediated decrease in MutS protein homolog 2 (MSH2) expression. (f) Decreased MSH2 expression is observed in glioma cells upon siRNA-mediated EZH2 knockdown. Blots (a, b, d–f) are representative images of three independent experiments ($n = 3$) showing similar results. Blots were stripped and re-probed for β-actin or c23 to establish equivalent loading.

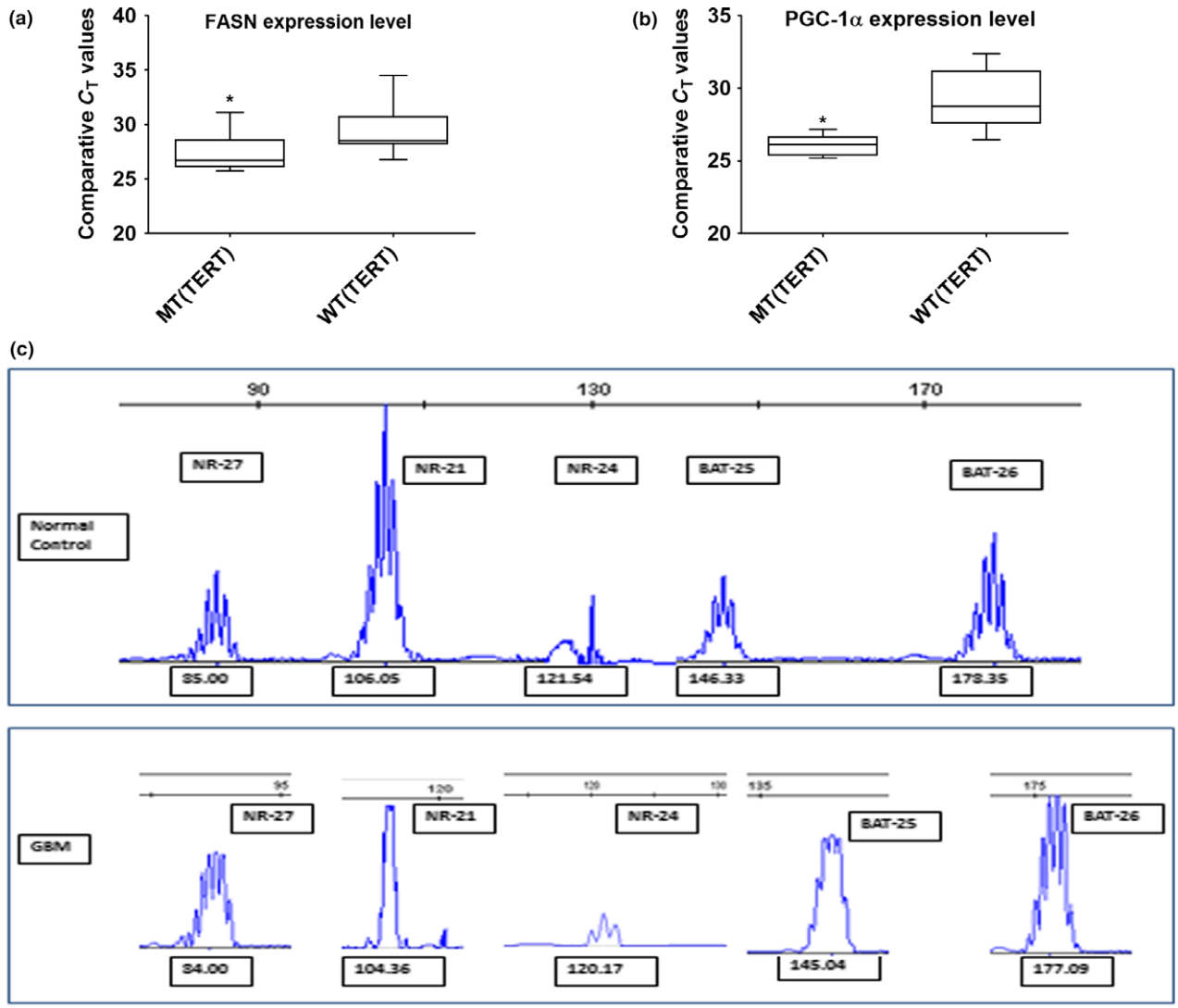

Fig. 5 Increased expression of fatty acid synthase (FASN) and peroxisome proliferator-activated receptor gamma coactivator 1-alpha (PGC-1α) is concomitant with high microsatellite instability (MSI) in telomerase reverse transcriptase (TERT) promoter mutant glioblastoma (GBM). qRT-PCR shows an increase in (a) FASN and (b) PGC-1α transcript levels in C228T- and C250T-mutated (MT) (n = 12) tumor samples as compared to wild-type (WT) (n = 13) tumor samples. Results were analyzed using Mann–Whitney test ($p < 0.05$). (c) MSI analysis in GBM patient samples. About 30% of the tumors bearing human TERT promoter mutations were found to be MSI positive when compared to controls. In contrast, only 10% of wild-type tumors were MSI positive.

of telomeres (Bechter *et al.* 2004), but telomerase activation is also frequent in tumors exhibiting MSI (Ibanez de Caceres *et al.* 2004) resulting from a failure of the MMR system. As FASN over-expression has been associated with MSI in colorectal cancer (Ogino *et al.* 2007), the altered status of MSH2 in TERT mutants could account for heightened MSI in these mutants with dysregulated lipid metabolism. Interestingly, telomere instability occurs in MSI-high tumors and is more common than in microsatellite stable cancers (Pickett *et al.* 2004). Based on our findings, it seems likely that responsiveness to therapeutic interventions targeting EZH2–TERT–lipid metabolism association in GBM may yield differential responses depending on the status of both TERT promoter mutations and MSI.

This study provides better understanding of aberrant metabolic programming in GBM based on distinctive genetic alterations. From a translational point of view, comprehensive characterization of GBM tumors based on their molecular properties such as genetic alterations, lipid accumulation, microsatellite instability, and histone marks might redefine therapeutic regimens for GBM. Therapeutic strategies aimed at disrupting EZH2–TERT–lipid metabolism interplay are likely to exhibit inherent specificity for TERT mutant as compared to TERT wild-type GBM tumors.

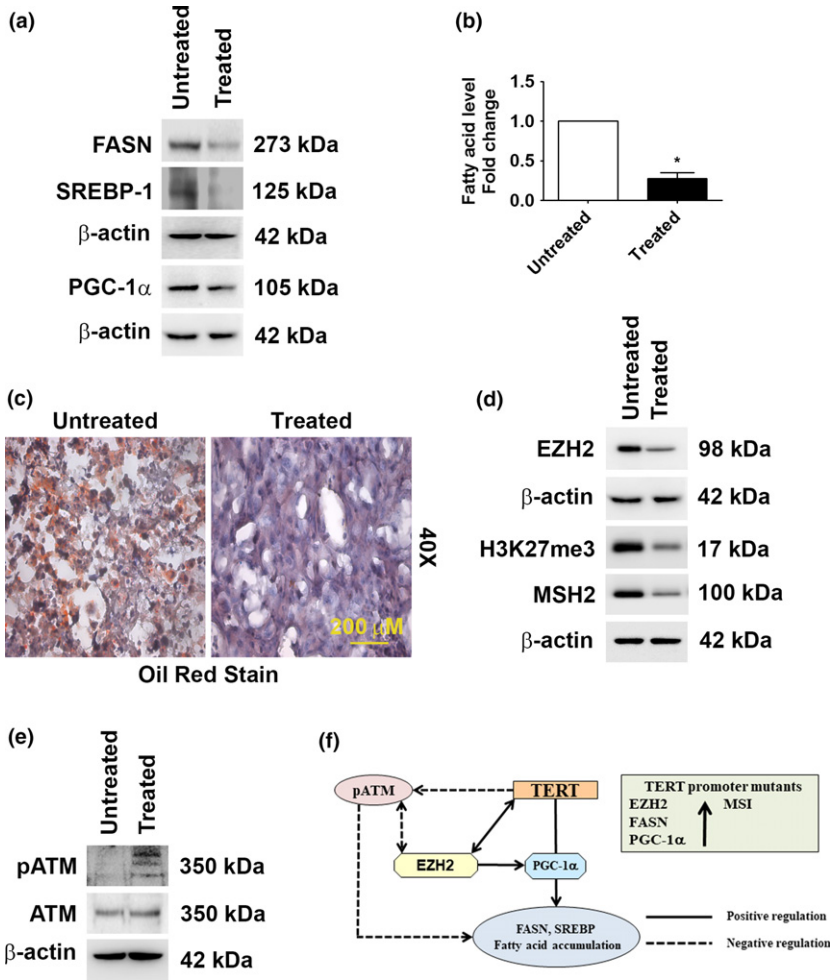

Fig. 6 Costunolide inhibits fatty acid synthase and its regulators in heterotypic xenograft glioma model. (a) Western blot images showing decreased fatty acid synthase (FASN), sterol regulatory element-binding protein-1 (SREBP-1), and peroxisome proliferator-activated receptor gamma coactivator 1-alpha (PGC-1α) levels in costunolide-treated tumor xenograft as compared to untreated tumor xenograft tissue. (b) Costunolide decreases fatty acid levels in tumor xenograft tissue. Values in the graph indicate means ± SEM ($n = 4$). Statistical analysis was done using unpaired Student's *t*-test ($p < 0.05$). * denotes significant change from the untreated group. (c) Oil red staining demonstrates decreased accumulation of lipid droplets in costunolide-treated tumor xenograft as compared to untreated tumor xenograft. Representative images from animals of each group are shown ($n = 4$). (d) Immunoblots showing reduced levels of enhancer of zeste homolog 2 (EZH2), H3K27me3, and MutS protein homolog 2 (MSH2) in costunolide-treated tumor xenograft as compared to untreated tumor xenograft. (e) Immunoblot depicting elevated phosphorylated ATM levels in cell lysates from costunolide-treated tumor xenograft as compared to untreated tumor xenograft. Blots (a, d, and e) are representative images of ($n = 6$) independent experiments showing similar results. Blots were stripped and re-probed for β-actin to establish equivalent loading. (f) Proposed model explaining the non-canonical function of TERT and the role of TERT-EZH2 network in the regulation of lipid metabolism and DNA damage response.

Acknowledgments and conflict of interest disclosure

FA is supported by a research fellowship from DBT, Government of India. The technical assistance of Rajesh Kumar Kumawat is acknowledged. The work was supported by a research grant from the Department of Biotechnology (DBT, Government of India #BT/ Med/ 30/SP11016/2015) to ES. The authors declare no conflict of interest.

All experiments were conducted in compliance with the ARRIVE guidelines.

Supporting information

Additional Supporting Information may be found online in the supporting information tab for this article:

Figure S1. Expression of FASN and SREBP-1 in glioma cells is TERT dependent.

Figure S2. PGC-1α regulates FASN level.

Figure S3. Betulin induces glioma cell apoptosis.

Figure S4. Lipid metabolism as H3K27me3 target in TERT-mutant GBM.

Figure S5. TERT regulates EZH2 and vice versa to affect fatty acid metabolism in glioma cells.

Figure S6. Counter-regulatory effect of ATM on TERT-driven FASN and MSH2 expressions in glioma cells.

Figure S7. Elevated lipid accumulation and increased MSH2 expression in TERT-mutant GBM.

Figure S8. Greater genomic instability in gliomas harboring TERT promoter mutation.

Figure S9. Diminished expression of fatty acid synthase and its regulators in costunolide-treated xenografts.

Table S1. H3K27me3 targets in TERT wild-type and mutant groups found differentially regulated.

Table S2. MSI analysis in TERT-mutant (MT) and wild-type (WT) gliomas.

References

Ahmad F., Dixit D., Sharma V., Kumar A., Joshi S. D., Sarkar C. and Sen E. (2016) Nrf2-driven TERT regulates pentose phosphate pathway in glioblastoma. *Cell Death Dis.* **7**, e2213.

Bechter O. E., Zou Y., Walker W., Wright W. E. and Shay J. W. (2004) Telomeric recombination in mismatch repair deficient human colon cancer cells after telomerase inhibition. *Cancer Res.* **64**, 3444–3451.

Blasco M. A. (2005) Telomeres and human disease: ageing, cancer and beyond. *Nat. Rev. Genet.* **6**, 611–622.

Campbell S., Ismail I. H., Young L. C., Poirier G. G. and Hendzel M. J. (2013) Polycomb repressive complex 2 contributes to DNA double-strand break repair. *Cell Cycle* **12**, 2675–2683.

Cao R., Wang L., Wang H., Xia L., Erdjument-Bromage H., Tempst P., Jones R. S. and Zhang Y. (2002) Role of histone H3 lysine 27 methylation in Polycomb-group silencing. *Science* **298**, 1039–1043.

Chang C. J., Yang J. Y., Xia W., Chen C. T., Xie X., Chao C. H., Woodward W. A., Hsu J. M., Hortobagyi G. N. and Hung M. C. (2011) EZH2 promotes expansion of breast tumor initiating cells through activation of RAF1-beta-catenin signaling. *Cancer Cell* **19**, 86–100.

Cosentino C., Grieco D. and Costanzo V. (2011) ATM activates the pentose phosphate pathway promoting anti-oxidant defence and DNA repair. *EMBO J.* **30**, 546–555.

Dixit D., Sharma V., Ghosh S., Koul N., Mishra P. K. and Sen E. (2009) Manumycin inhibits STAT3, telomerase activity, and growth of glioma cells by elevating intracellular reactive oxygen species generation. *Free Radic. Biol. Med.* **47**, 364–374.

Dixit D., Sharma V., Ghosh S., Mehta V. S. and Sen E. (2012) Inhibition of Casein kinase-2 induces p53-dependent cell cycle arrest and sensitizes glioblastoma cells to tumor necrosis factor (TNFalpha)-induced apoptosis through SIRT1 inhibition. *Cell Death Dis.* **3**, e271.

Flavin R., Peluso S., Nguyen P. L. and Loda M. (2010) Fatty acid synthase as a potential therapeutic target in cancer. *Future Oncol.* **6**, 551–562.

Floer M., Binion D. G., Nelson V. M. *et al.* (2008) Role of MutS homolog 2 (MSH2) in intestinal myofibroblast proliferation during Crohn's disease stricture formation. *Am. J. Physiol. Gastrointest. Liver Physiol.* **295**, G581–G590.

Ghosh S., Paul A. and Sen E. (2013) Tumor necrosis factor alpha-induced hypoxia-inducible factor 1alpha-beta-catenin axis regulates major histocompatibility complex class I gene activation through chromatin remodeling. *Mol. Cell. Biol.* **33**, 2718–2731.

Goel A., Nagasaka T., Hamelin R. and Boland C. R. (2010) An optimized pentaplex PCR for detecting DNA mismatch repair-deficient colorectal cancers. *PLoS ONE* **5**, e9393.

Grube S., Dunisch P., Freitag D., Klausnitzer M., Sakr Y., Walter J., Kalff R. and Ewald C. (2014) Overexpression of fatty acid synthase in human gliomas correlates with the WHO tumor grade and inhibition with Orlistat reduces cell viability and triggers apoptosis. *J. Neurooncol.* **118**, 277–287.

Hu S., Yu L., Li Z., Shen Y., Wang J., Cai J., Xiao L. and Wang Z. (2010) Overexpression of EZH2 contributes to acquired cisplatin resistance in ovarian cancer cells in vitro and in vivo. *Cancer Biol. Ther.* **10**, 788–795.

Huang W. C., Li X., Liu J., Lin J. and Chung L. W. (2012) Activation of androgen receptor, lipogenesis, and oxidative stress converged by SREBP-1 is responsible for regulating growth and progression of prostate cancer cells. *Mol. Cancer Res.* **10**, 133–142.

Huang F. W., Hodis E., Xu M. J., Kryukov G. V., Chin L. and Garraway L. A. (2013) Highly recurrent TERT promoter mutations in human melanoma. *Science* **339**, 957–959.

Ibanez de Caceres I., Frolova N., Varkonyi R. J., Dulaimi E., Meropol N. J., Broccoli D. and Cairns P. (2004) Telomerase is frequently activated in tumors with microsatellite instability. *Cancer Biol. Ther.* **3**, 289–292.

Kather H., Rivera M. and Brand K. (1972) Interrelationship and control of glucose metabolism and lipogenesis in isolated fat-cells. Control of pentose phosphate-cycle activity by cellular requirement for reduced nicotinamide adenine dinucleotide phosphate. *Biochem. J.* **128**, 1097–1102.

Killela P. J., Reitman Z. J., Jiao Y. *et al.* (2013) TERT promoter mutations occur frequently in gliomas and a subset of tumors derived from cells with low rates of self-renewal. *Proc. Natl Acad. Sci. USA* **110**, 6021–6026.

Kim E., Kim M., Woo D. H. *et al.* (2013) Phosphorylation of EZH2 activates STAT3 signaling via STAT3 methylation and promotes tumorigenicity of glioblastoma stem-like cells. *Cancer Cell* **23**, 839–852.

Kleer C. G., Cao Q., Varambally S. *et al.* (2003) EZH2 is a marker of aggressive breast cancer and promotes neoplastic transformation of breast epithelial cells. *Proc. Natl Acad. Sci. USA* **100**, 11606–11611.

Li J., Hart R. P., Mallimo E. M., Swerdel M. R., Kusnecov A. W. and Herrup K. (2013) EZH2-mediated H3K27 trimethylation mediates neurodegeneration in ataxia-telangiectasia. *Nat. Neurosci.* **16**, 1745–1753.

Li Y., Zhou Q. L., Sun W. *et al.* (2015) Non-canonical NF-kappaB signalling and ETS1/2 cooperatively drive C250T mutant TERT promoter activation. *Nat. Cell Biol.* **17**, 1327–1338.

Martinez P., Siegl-Cachedenier I., Flores J. M. and Blasco M. A. (2009) MSH2 deficiency abolishes the anticancer and pro-aging activity of short telomeres. *Aging Cell* **8**, 2–17.

McFaline-Figueroa J. L., Braun C. J., Stanciu M. *et al.* (2015) Minor changes in expression of the mismatch repair protein MSH2 exert a major impact on glioblastoma response to temozolomide. *Cancer Res.* **75**, 3127–3138.

Mehlem A., Hagberg C. E., Muhl L., Eriksson U. and Falkevall A. (2013) Imaging of neutral lipids by oil red O for analyzing the metabolic status in health and disease. *Nat. Protoc.* **8**, 1149–1154.

Natsume A., Ito M., Katsushima K. *et al.* (2013) Chromatin regulator PRC2 is a key regulator of epigenetic plasticity in glioblastoma. *Cancer Res.* **73**, 4559–4570.

Ogino S., Kawasaki T., Ogawa A., Kirkner G. J., Loda M. and Fuchs C. S. (2007) Fatty acid synthase overexpression in colorectal cancer is associated with microsatellite instability, independent of CpG island methylator phenotype. *Hum. Pathol.* **38**, 842–849.

Orzan F., Pellegatta S., Poliani P. L., Pisati F., Caldera V., Menghi F., Kapetis D., Marras C., Schiffer D. and Finocchiaro G. (2011) Enhancer of Zeste 2 (EZH2) is up-regulated in malignant gliomas and in glioma stem-like cells. *Neuropathol. Appl. Neurobiol.* **37**, 381–394.

Pang B., Zheng X. R., Tian J. X., Gao T. H., Gu G. Y., Zhang R., Fu Y. B., Pang Q., Li X. G. and Liu Q. (2016) EZH2 promotes metabolic reprogramming in glioblastomas through epigenetic repression of EAF2-HIF1alpha signaling. *Oncotarget* **7**, 45134–45143.

Pickett H. A., Baird D. M., Hoff-Olsen P., Meling G. I., Rognum T. O., Shaw J., West K. P. and Royle N. J. (2004) Telomere instability detected in sporadic colon cancers, some showing mutations in a mismatch repair gene. *Oncogene* **23**, 3434–3443.

Podrini C., Koffas A., Chokshi S., Vinciguerra M., Lelliott C. J., White J. K., Adissu H. A., Williams R. and Greco A. (2015) MacroH2A1 isoforms are associated with epigenetic markers for activation of lipogenic genes in fat-induced steatosis. *FASEB J.* **29**, 1676–1687.

Pucci F., Gardano L. and Harrington L. (2013) Short telomeres in ESCs lead to unstable differentiation. *Cell Stem Cell* **12**, 479–486.

Sahin E., Colla S., Liesa M. *et al.* (2011) Telomere dysfunction induces metabolic and mitochondrial compromise. *Nature* **470**, 359–365.

Sharma V., Malgulwar P. B., Purkait S. *et al.* (2016) Genome-wide ChIP-seq analysis of EZH2-mediated H3K27me3 target gene profile highlights differences between low- and high-grade astrocytic tumors. *Carcinogenesis* **38**, 152–161.

Sparmann A. and van Lohuizen M. (2006) Polycomb silencers control cell fate, development and cancer. *Nat. Rev. Cancer* **6**, 846–856.

Stern J. L., Theodorescu D., Vogelstein B., Papadopoulos N. and Cech T. R. (2015) Mutation of the TERT promoter, switch to active chromatin, and monoallelic TERT expression in multiple cancers. *Genes Dev.* **29**, 2219–2224.

Summermatter S., Baum O., Santos G., Hoppeler H. and Handschin C. (2010) Peroxisome proliferator-activated receptor gamma coactivator 1{alpha} (PGC-1{alpha}) promotes skeletal muscle lipid refueling in vivo by activating de novo lipogenesis and the pentose phosphate pathway. *J. Biol. Chem.* **285**, 32793–32800.

Tewari R., Choudhury S. R., Ghosh S., Mehta V. S. and Sen E. (2012) Involvement of TNFalpha-induced TLR4-NF-kappaB and TLR4-HIF-1alpha feed-forward loops in the regulation of inflammatory responses in glioma. *J. Mol. Med. (Berl)* **90**, 67–80.

Trautmann K., Terdiman J. P., French A. J. *et al.* (2006) Chromosomal instability in microsatellite-unstable and stable colon cancer. *Clin. Cancer Res.* **12**, 6379–6385.

Varambally S., Dhanasekaran S. M., Zhou M. *et al.* (2002) The polycomb group protein EZH2 is involved in progression of prostate cancer. *Nature* **419**, 624–629.

Wakamiya T., Suzuki S. O., Hamasaki H., Honda H., Mizoguchi M., Yoshimoto K. and Iwaki T. (2014) Elevated expression of fatty acid synthase and nuclear localization of carnitine palmitoyltransferase 1C are common among human gliomas. *Neuropathology* **34**, 465–474.

Wallace M. and Metallo C. M. (2016) PGC1alpha drives a metabolic block on prostate cancer progression. *Nat. Cell Biol.* **18**, 589–590.

Xiao R., Su Y., Simmen R. C. and Simmen F. A. (2008) Dietary soy protein inhibits DNA damage and cell survival of colon epithelial cells through attenuated expression of fatty acid synthase. *Am. J. Physiol. Gastrointest. Liver Physiol.* **294**, G868–G876.

Xiong S., Patrushev N., Forouzandeh F., Hilenski L. and Alexander R. W. (2015) PGC-1alpha modulates telomere function and DNA damage in protecting against aging-related chronic diseases. *Cell Rep.* **12**, 1391–1399.

Yang Q., Laknaur A., Elam L., Ismail N., Gavrilova-Jordan L., Lue J., Diamond M. P. and Al-Hendy A. (2016) Identification of polycomb group protein EZH2-mediated DNA mismatch repair gene MSH2 in human uterine fibroids. *Reprod. Sci.* **23**, 1314–1325.

Yasumoto Y., Miyazaki H., Vaidyan L. K. *et al.* (2016) Inhibition of fatty acid synthase decreases expression of stemness markers in glioma stem cells. *PLoS ONE* **11**, e0147717.

Zeng L., Wu G. Z., Goh K. J. *et al.* (2008) Saturated fatty acids modulate cell response to DNA damage: implication for their role in tumorigenesis. *PLoS ONE* **3**, e2329.

